Chapter 6

# Structure-Property Correlations and Superconductivity in Spinels

Weiwei Xie and Huixia Luo

Additional information is available at the end of the chapter

http://dx.doi.org/10.5772/65943

**Abstract**

In this chapter, alternative views based on the structure have been presented in the spinel superconducting compounds, including the only oxide spinel superconductor, $LiTi_2O_4$, and non-oxide superconductors, $CuIr_2S_4$ and $CuV_2S_4$. Inspection of the atomic arrangements, electronic structures and bonding interactions of spinel superconductor, $LiTi_2O_4$ shows that $LiTi_2O_4$ can be interpreted as Li-doped $TiO_2$, which is similar with doping Cu into $TiSe_2$ to induce superconductivity. Different from $LiTi_2O_4$, the electronic structures of $CuIr_2S_4$ and $CuV_2S_4$ indicate a distinctive way to understand them in the structural viewpoint. The $d^6$ electron configuration and the octahedral coordination of Ir in $CuIr_2S_4$ can be analogous to the $d^6$ in perovskites, which sometimes host a metal-insulator transition. However, the superconductivity in $CuV_2S_4$ may be induced from the suppression of charge density waves. This kind of structural views will help chemists understand physical phenomena obviously more straightforward, though not sufficient, as clearly shown by the competition between each other, such as superconductivity and other structural phase transition (CDWs), oxidation fluctuation or magnsetism.

**Keywords:** superconductivity, chemical bonding, crystal structural analysis

## 1. Introduction

Superconducting phenomenon incorporates the exact zero electrical resistance and expulsion of magnetic flux fields occurring in many solid state materials when cooling below a certain critical temperature [1]. The expulsion of the magnetic flux fields, known as Meissner effect, and zero electric resistance has tremendous applications in the fields of transportation, electricity, and so on [2]. The "ideal" superconducting materials potentially could solve the most energy problems human being is facing. Back to the discovery

of superconductivity in mercury in 1911, a century has passed by. However, the mechanisms of superconductivity are still undergoing extraordinary scrutiny. The conventional pictures arising from the Bardeen-Cooper-Scrieffer (BCS) theory merge the electron-phonon coupling to generate a pairing mechanism between electrons with the opposite crystal momenta that induce a superconducting state [3,4]. Derived from the BCS theory, the qualitative correlation between the superconducting critical temperature ($T_c$) and the density of states (DOS) at the Fermi level, $N(E_F)$, is $kT_c = 1.13\ \hbar\ \omega\ \exp(-1/N(E_F)V)$, where V is a merit of the electron-phonon interaction and $\omega$ is a characteristic phonon frequency, similar to the Debye frequency [5]. According to the expression, a large density of states at Fermi level $N(E_F)$ or electron-phonon interaction V or both leads to a higher $T_c$ superconductor. Later, Eliashberg and McMillan extended the BCS theory and gave a better correspondence between experiment and prediction [6].

Until now, BCS theory is still in an even more dominant position to determine whether a superconductor will be classified as BCS-like or not. As more high temperature superconductors were discovered, more new "universal" mechanisms were sought for. However, neither BCS nor other exotic mechanisms established a relationship with the real chemical systems. Thus, the question appears whether the general statements of BCS theory can be associated with distinct chemical meanings, such as specific bonding situations, and whether the physical phenomenon of superconductivity can be interpreted from the viewpoint of chemistry.

## 2. Electron counting rules in chemistry and superconductors

Empirical observations of the range of electron counts to specific structural compounds are widely used in chemistry to help determine and find out the empirical rules to stabilize the compounds with specific structural frameworks, such as Wades-Mingo polyhedral skeletal rules for boron cluster compounds [7], $14e^-$ rules for DNA-like helix Chimney Ladders phases [8] and Hume-Rothery rules for multi-shelled clustering $\gamma$-brass phases [9, 10]. The electronic structure calculation and the bonding schemes allow us to determine a structure's preferred electron count for most compounds, for example, take Hume-Rothery rules in complex clustering compounds. The stability ranges of complex intermetallic alloys (CMAs) are frequently identified by specific valence electron-to-atom ($e/a$) ratios, such as 1.617 e-/a for transition-metal-free $\gamma$-brass systems, which are generally called Hume-Rothery rules and validated by the presence of pseudogaps at the corresponding Fermi level in the calculated electronic structures [10]. Moreover, a distinctive way to count electrons is applied for the transition-metal-rich systems, such as Chimney Ladders phases, endohedral gallides superconductors, and so on [11]. For example, Ga-cluster superconductor, $ReGa_5$, containing 11 bonding orbitals in the cluster would be fully occupied by 22e- (Re: 7e- from 5*d* and 6*s* orbitals + 5Ga: 3e- from 4*s* and 4*p* orbitals) and the Fermi level of $ReGa_5$ should be located in a gap or pseudo gap in the DOS [11]. Briefly, small values of density of states, $N(E_F)$, are corresponding to the stable electronic structures in the reciprocal space and chemical compounds in the real chemistry system [12]. As we mentioned in early section, $N(E_F)$ exists the

http://dx.doi.org/10.5772/65943

close relationship with the superconducting critical temperatures: the larger values of $N(E_F)$ in DOS, the higher $T_c$ is likely to appear in the solid state materials. An empirical electron counting method, although this follows a different, less chemical-based electron counting process, was generated by Matthias [13]. It states that the number of valence electrons in a superconductor has lost nothing of its fundamental importance to the value of $T_c$. For the transition-metal-rich compounds with simple crystal structures, the maximum in $T_c$ is seen to occur at approximately 4.7 and 6.5 valence electrons per atom [14]. The particular impressive example is the $T_c$ dependence on the average number of valence electrons in A15 phases, for example, take $Nb_3Ge$. The valence electron concentration is calculated as follows: (5 e-/Nb × 3 Nb + 4 e-/Ge × 1 Ge)/4 = 4.75 e-/atom [15]. Similarly, 4.6 e-/atom work for $(Zr/Hf)_5Sb_{2.5}Ru_{0.5}$ [16, 17]. Therefore, to increase the $T_c$ in superconductivity is at a high risk of destabilizing the compounds. From the chemistry viewpoints, BCS-like superconductors need to balance the structural stability and superconducting property and result in the limited $T_c$ [18]. Circumventing the inherent conflict of structural stability and superconducting critical temperatures in BCS-like superconductors would be analogous to the thermoelectric materials with a phonon glass with electron-crystal properties [19].

In the past several decades, several new classes of high temperature superconductors were discovered, whose critical temperatures are way above the ones of conventional superconductors [20–23]. These discoveries give physicists hope to keep looking for the new mechanisms for superconductivity. Different from metallic superconductors, more chemistry terms can be applied for the high temperature superconductors, such as oxidation numbers, Zintl phases, valence-electron-precise systems, and so on [24, 25].

## 3. Inducing superconductivity by the suppression of charge density waves

In the semiconductor $BaBiO_3$ compound, the bonding interaction can be described by the formula $(Ba^{2+})(Bi^{4+})(O^{2-})_3$, Bi has the unusual oxidation state, +IV [26, 27]. At room temperature, it has the doubled perovskite unit cell and the structure distorted to monoclinic rather than being cubic. It contains two types of Bi atoms in different sized coordinated polyhedral, so the formula of $BaBiO_3$ can be modified as $(Ba^{2+})_2(Bi^{3+})(Bi^{5+})(O^{2-})_6$. Now the complex structural distortion can be interpreted as the relocalization of two electrons at the $Bi^{3+}$ ion with the "long pair" configuration [28]. Contradictory, the two Bi atoms show slightly different in the oxidation states (+3.9 versa +4.1) from the band structure calculation [29]. Another argument was arisen that the structural distortion, as well as the non-equivalent Bi atoms, caused by the charge density waves (CDWs) [30]. Suppression of the charge density waves in Bi oxides may induce the superconductivity. It is achieved by doping $Pb^{4+}$, which has closed electron configuration and prefers a regularly coordinated environment to stabilize the structure. $BaPb_xBi_{1-x}O_{3-\delta}$ shows no CDWs but the superconducting transition when cooling to 13 K [31]. Another way to stabilize the regular structure is increasing the $Bi^{5+}$ ions, which also has the closed electron configuration. To obtain this, K was used to partially replace Ba and $K_xBa_{1-x}BiO_3$ in cubic perovskite structure shows the superconducting transition around 30 K [26].

## 4. Superconductivity hosted in the specific structural frameworks

High temperature superconductivity in $ThCr_2Si_2$-type iron pnictides led to numerous investigations in these compounds in the past decade [32]. However, the structure of $ThCr_2Si_2$-type materials hosting superconductivity could be traced back to the quaternary superconductors, $LnNi_2B_2C$ (Ln = Ho, Er, Tm, Y and Lu) [33]. In $LnNi_2B_2C$, we could treat the B-C-B as a single chemical unit based on the short bonding distance and strong bonding interaction between B and C [34]. Therefore, the ionic formula of $LnNi_2B_2C$ can be treated as $Ln^{3+}(Ni^0)_2(B_2C)^{3-}$ [34]. In the viewpoint of chemistry, the large $N(E_F)$ in $LnNi_2B_2C$ was mainly arisen from the slight orbital distortion of B-C-B fragments. Moreover, the structure could be considered to represent the first member of a homologous series $(LnC)_n(Ni_2B_2)$, in which the LnC block adopts to a NaCl-type packing, which naturally drove us to investigate the $(LnC)_2(Ni_2B_2)$, written as (LnC)(NiB), in which the ionic formula could be written as $Ln^{3+}(Ni^0)(BC)^{3-}$ [33]. $(BC)^{3-}$ is isoelectronic with CO, and the B-C interaction rapidly changes from bonding to antibonding in addition to the dispersionless band from Ln orbital below Fermi level in LnNiBC may be the important factor to kill the superconductivity [34].

However, the "exotic" quantum mechanism for superconductivity is undergoing an unclear status even though the phenomenon has been discovered for more than a century. Superconductivity is still unpredictable currently. Condensed matter physicists try to predict superconductors based on analyzing the superconductivity through "*k*-space" pictures based on Fermi surfaces and particles interactions, that is, electron-phonon coupling [35]. Thus, there are few predictive rules from physics aspect, one of which, perhaps the most widely used, is that in intermetallic compounds of a known superconducting structure type, one can count electrons and expect to find the best superconductivity or the highest critical temperature ($T_c$) at ~4.7 or ~6.5 valence electrons per atom—Matthias rules mentioned above [14]. However, the chemists' viewpoint is from real space such as chemical compositions and atomic structures, which play critical roles in superconductivity, rather than reciprocal space [11]. One of the chemical views to increase the occurrence of new superconducting materials is to posit that it carries out in structural families. The well-known examples are found in $ThCr_2Si_2$-type such as $BaFe_2As_2$ and $LnNi_2B_2C$ systems and perovskites like bismuth oxides, which are fairly favored by superconductivity [32]. Laves phase compounds are previously well-investigated families for hosting superconductivity among alloys [36]. Here, we analyze the structural relationship between diamond framework and spinels from a molecular perspective, then apply this connection for interpretation and prediction of other possible new superconductors adopting to spinels and their derived structures.

## 5. Calculation details

### 5.1. Tight-binding, linear Muffin-Tin orbital-atomic spheres approximation (TB-LMTO-ASA)

Calculations of the electronic structures were performed by TB-LMTO-ASA using the Stuttgart code [37–39]. Exchange and correlation were treated by the local density approximation

(LDA) [40]. In the ASA method, space is filled with overlapping Wigner-Seitz (WS) spheres [41]. The symmetry of the potential is considered spherical inside each WS sphere, and a combined correction is used to take into account the overlapping part, and the overlap of WS spheresis limited to no larger than 16%. The empty spheres are necessary, and the overlap between empty spheres is limited to no larger than 40%.The convergence criterion was set to 0.1 meV.A mesh of ~100 *k* points [42] in the irreducible edge of the first Brillouin zone was used to obtain all integrated values, including the density of states (DOS) and Crystal Orbital Hamiltonian Population (COHP) curves [43].

### 5.2. WIEN2k

The electronic structures (density of states and band structure) of intermetallics were calculated using the WIEN2k code with spin orbital coupling, which has the full-potential linearized augmented plane wave method (FP-LAPW) with local orbitals implemented [44, 45]. For the treatment of the electron correlation within the generalized gradient approximation, the electron exchange-correlation potential was used with the parameterization by Perdew et al. (i.e. the PBE-GGA) [46]. For valence states, relativistic effects were included through a scalar relativistic treatment, and core states were treated fully relativistic [47]. The structure used to calculate the band structure was based on the single crystal data. The conjugate gradient algorithm was applied, and the energy cutoff was 500 eV. Reciprocal space integrations were completed over a 9 × 9 × 9 Monkhorst-Pack *k*-points mesh with the linear tetrahedron method. With these settings, the calculated total energy converged to less than 0.1 meV per atom.

### 5.3. Materials projects

The electronic structures of partial hypothetical compounds were predicted and calculated using the Materials Projects, which have been treated in the electron correlation within the generalized gradient approximation. The structure used to calculate the band structure was based on the single crystal data. The conjugate gradient algorithm was applied, and the energy cutoff was 520 eV. Reciprocal space integrations were completed over a 104 Monkhorst-Pack *k*-points mesh with the linear tetrahedron method.

## 6. Hierarchical structural interpretation of existing superconductors with spinels

Spinels, generally formulated as $A^{2+}(B^{3+})_2O_4$, crystallize in the cubic crystal system, with the oxide anions arranged in a cubic close-packed lattice and the cations A and B occupy the octahedral and tetrahedral sites in the lattice [48, 49]. An alternative tantalizing way to view the spinel structure is to treat spinels as void-filled cubic Laves phases, both of which exhibit some close relationships with the diamond structure. In the cubic Laves phase, $MgCu_2$, the Mg atom sites (Wyckoff designation 8*a*) arrange precisely into a three-dimensional (3D) diamond network. Within the voids, Cu atoms (Wyckoff designation 16*d*) form a 3D framework of vertex-sharing tetrahedra, as emphasized in **Figure 1** (Left). Thus, the Mg and Cu sites become A and B, respectively, in spinels. Furthermore, in spinels, the O atoms on 32*e* (*x*, *x*, *x*)

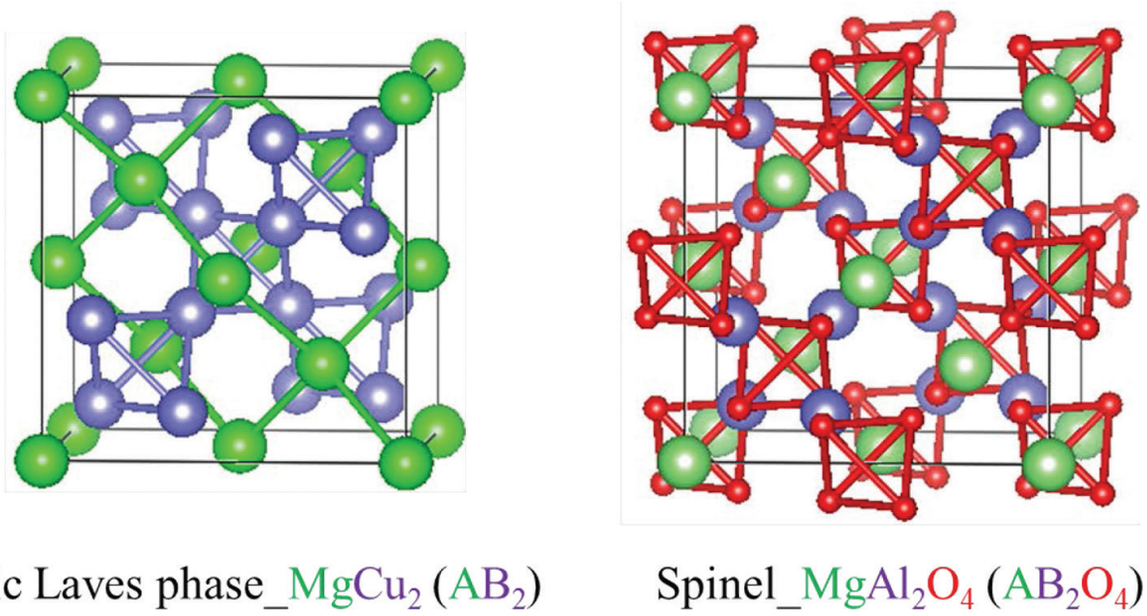


**Figure 1.** The structural relationship between the $MgCu_2$-type, cubic Laves phase structure and the spinel-type, $MgAl_2O_4$. *Left*: $MgCu_2$-type (Mg, green; Cu, purple); *right*: Spinel type $MgAl_2O_4$ (Mg, green; Al, purple and O, red).

sites forming isolated tetrahedral were inserted into the $B_4$ tetrahedra and center around 8*b* (½, ½, ½) sites in **Figure 1** (Right). The formation of the complete cubic unit cell from the cubic Laves phase to the spinels $A_8B_{16}O_{32}$ is, therefore, shown in **Figure 1**.

### 6.1. Li-doped "$TiO_2$": superconductivity in spinel $LiTi_2O_4$

Superconductivity in $Li_{1-x}Ti_{2+x}O_4$ was first reported in 1973, much earlier than the discovery of high-$T_c$ cuprate superconductors. The superconducting transition temperature ($T_c$) of $LiTi_2O_4$ is around 11 K [50]. As the first oxide superconductor with a relatively high critical temperature, $LiTi_2O_4$ remains widely intriguing for scientists. The most frequent questions arose are why $LiTi_2O_4$ adopts to a unique structure type, which is different from other high temperature superconducting materials, such as perovskites or cuprates. However, Li-doped $TiO_2$ and $LiTi_2O_4$ can be treated as the analogy between Cu-doped $TiSe_2$ and $Cu_{0.08}TiSe_2$ in a certain way [51]. $TiSe_2$ adopts to the trigonal-layered structure (1T) (S.G. P-31*m*) with charge density waves observed around 220 K, and with doping Cu, the superconductivity in $Cu_xTiSe_2$ appears and the charge density wave was suppressed. Similarly, for both rutile- and anatase-$TiO_2$, Ti and O atoms form distorted $Ti@O_6$ octahedra; thus, there exist empty voids in the structure shown in **Figure 2a** and **b**. Based on the electronic structures of $TiO_2$in **Figure 3a** and **b**, both polymorphic $TiO_2$ compounds are well-known *n*-type semiconductors with ~2eV gaps above Fermi levels [52]. Through doping with Li atom, which can be considered as the nearly free electron in solid state chemistry, the empty voids in $TiO_2$ are occupied by the Li atoms, and the Fermi levels start lifting up and shifting to the peak in the DOS.

To confirm our assumptions, the electronic structures of $LiTi_2O_4$ are calculated using TB-LMTO-ASA with Crystal Orbital Hamilton Population (COHP) codes. In **Figure 4** (left), the DOS

http://dx.doi.org/10.5772/65943

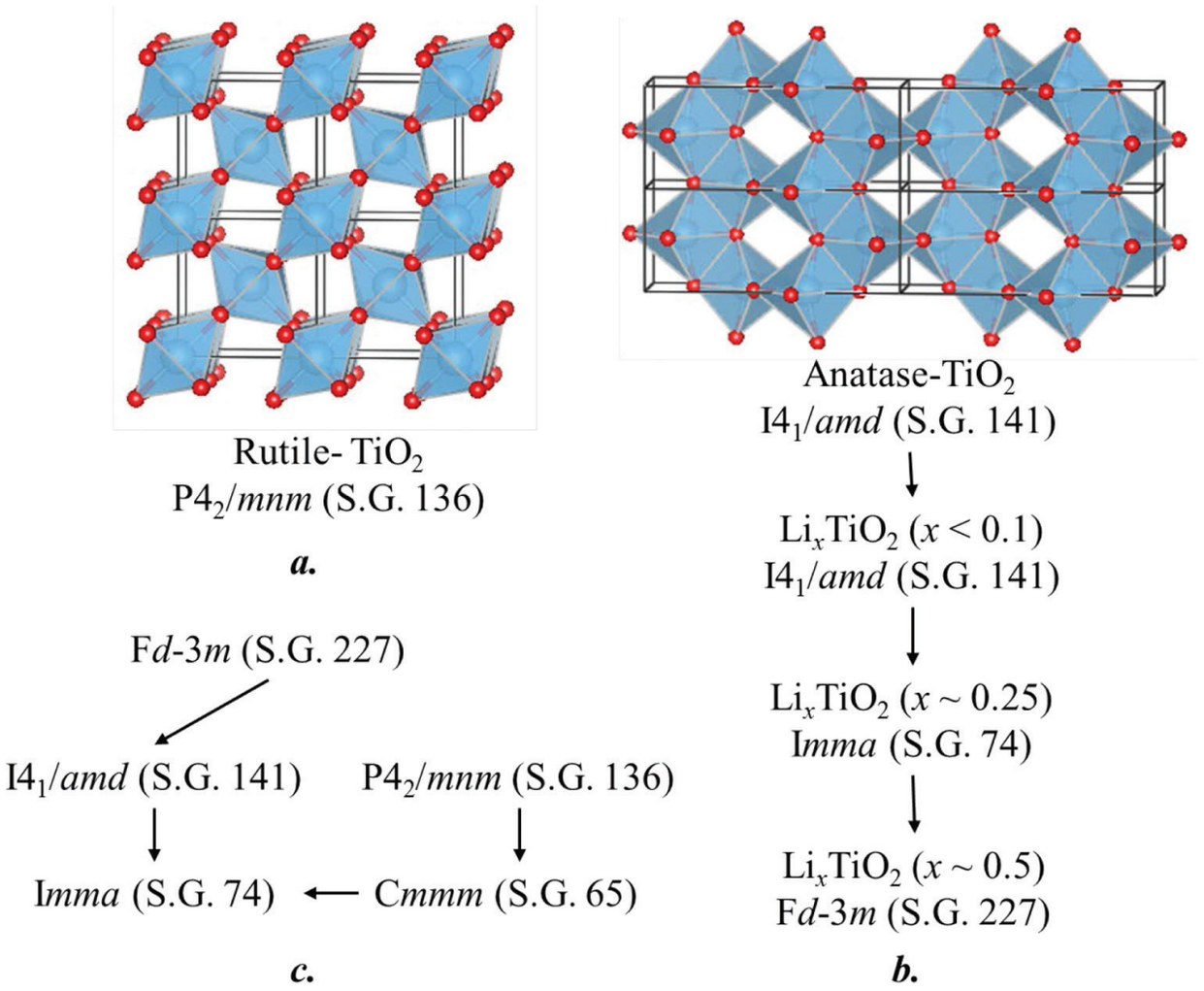


**Figure 2.** The structure and space group connections between two types of $TiO_2$ and $Li_xTiO_2$. (a) The crystal structure of rutile-$TiO_2$. The rutile-TiO2 adopts to the primitive tetragonal structure with space group $P4_2/mnm$. Each Ti atom surrounded by 6 O atoms forms the octahedral coordination. (b) The schematic picture showing the possible phase transitions when doping Li into $TiO_2$. (c) The space group and sub-space group relationship among $TiO_2$ and $LiTi_2O_4$.

qualitative features obtained by this calculation state that are 2–6 eV below the Fermi level ($E_F$) arise primarily from valence 4*s* and 3*d* orbitals from Ti and 2*p* orbitals from O, whereas the Li 2*s* band is broadly distributed from −6 to −2 eV. The contribution of Li 2*s* electrons to the DOS curve, as shaded in **Figure 4** in black, shows it just contributes one free electron to the system rather than making any change to the DOS features of $TiO_2$ in the diamond-like framework. The integrated DOS till the broad band gap around 1 eV below Fermi level results in the same electron counts as $TiO_2$. Comparing with the DOS of rutile- and anatase-$TiO_2$ in **Figure 3**, the difference between $LiTi_2O_4$ and $TiO_2$ is the up-lift 1 e- per formula of the Fermi level. The Fermi level for $LiTi_2O_4$ falls just above the topmost peak of the largely Ti 3*d* bands. Therefore, we employed Local Spin Density Approximation (LSDA) to see if a magnetic moment would spontaneously develop, but the converged result yielded zero magnetic moment. This result of the unstable electronic structure gives a strong indication of the occurrence of superconductivity. The "bond energy" term is evaluated by the crystal orbital Hamilton populations

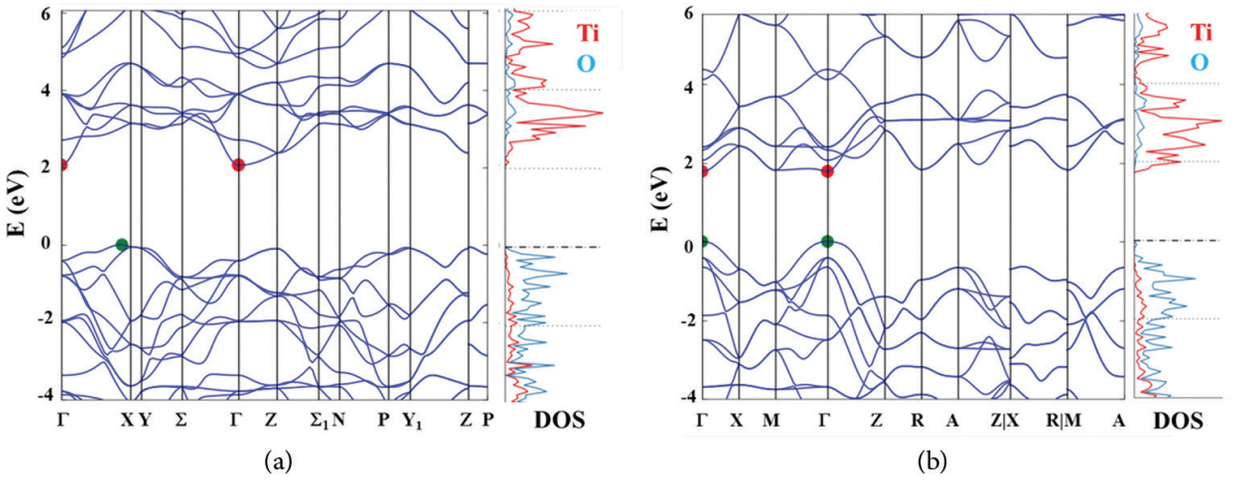


**Figure 3.** The band structures and density of states (DOS) of (a) anatase-$TiO_2$ with ~2eV indirect band gap and (b) rutile-$TiO_2$ with ~2eV direct band gap (generated from *Materials Projects*).

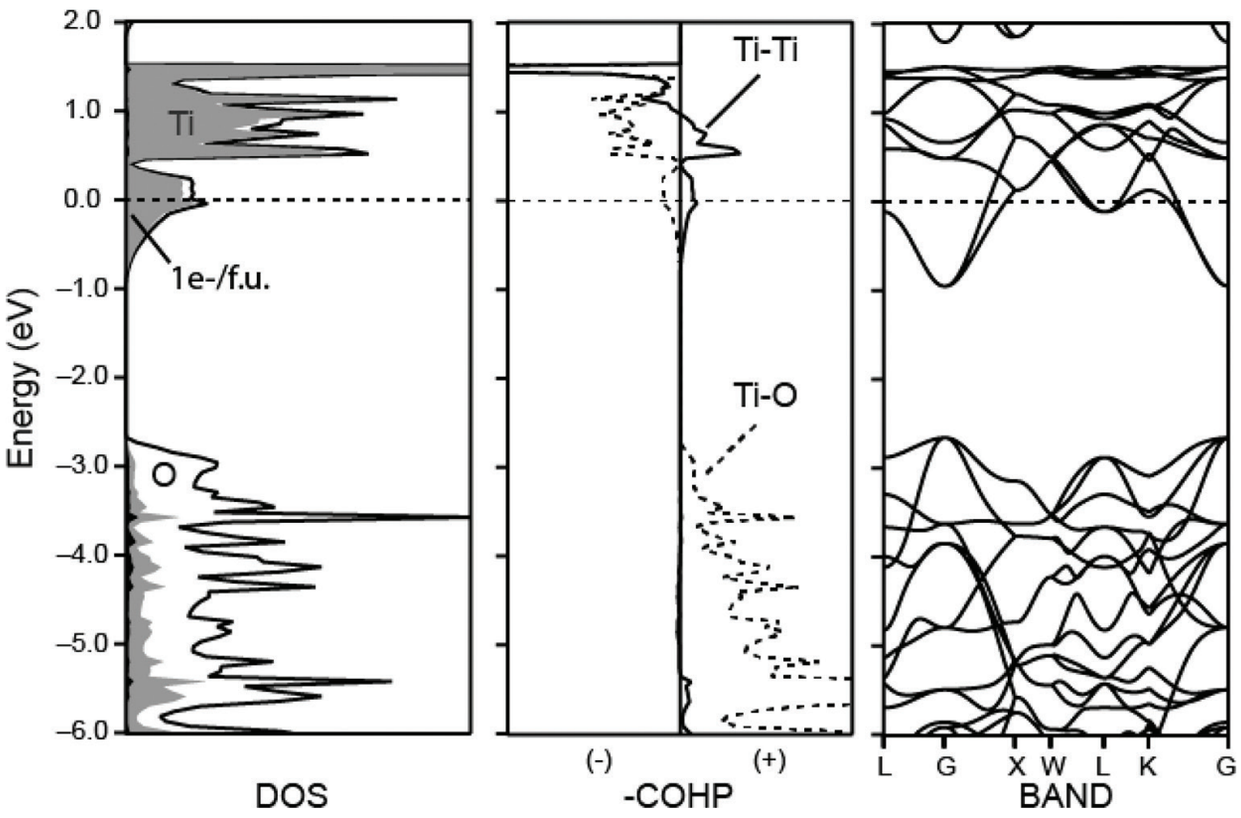


**Figure 4.** Electronic structure of spinel $LiTi_2O_4$. Partial DOS curves, –COHP curves and band structure of "$LiTi_2O_4$" obtained from non-spin-polarization (LDA). (+ is bonding/ – is anti-bonding).

(COHP) curves [53]. These curves illustrated in **Figure 4** (Middle) show that the band gap around 1eV below Fermi level corresponds to the non-bonding for the compound, similar in rutile- and anatase-$TiO_2$. Interestingly, there is no atomic interaction between Li and O or Li and Ti, which confirmed our claims discussed above—Li just acts as the electron-donator

to change the Fermi level as well as balance the charge, and empty sphere to fill the volume, rather than giving the impact on the electronic structure including changing the atomic interactions. In –COHP, the Fermi level is located on the Ti-O anti-bonding and Ti-Ti bonding interactions, the sum of the anti-bonding and bonding effects is close to zero, which indicates the possibility of the stabilization of the compound. The strong Ti–O antibonding interactions at the Fermi level, contributing the unstable factors in the electronic structure is significant relative with the superconductivity in spinel $LiTi_2O_4$. Meanwhile, in the band structure of spinel $LiTi_2O_4$, the Fermi level locates on the saddle points around U and W points in the Brillouin zone, which is a strong evidence for the unstable electronic structure.The structural connection might also be noted from the links between the space groups in **Figure 2**. If we divided the unit cell of the spinel structure into two along ½(***a*** + ***b***) and ½(***a*** - ***b***), the cubic structure will become tetragonal, and space group will decrease from F*d*-3m to $I4_1/amd$s. Furthermore, the distortion of ***a*** and ***b*** decreases the symmetry from tetragonal to orthorhombic and the space group will become I*mma* instead of $I4_1/amd$s. On the other side, I*mma* is also the direct subgroup of $P4_2/mnm$ (rutile-$TiO_2$). In summary, the structural transformation could be treated as the transition of a continuously doping Li process. When the amount of doped Li is small, the $Li_xTiO_2$ keeps in $I4_1/amd$s. As *x* increases, the orthorhombic structure appears. When *x* is close to 0.5, the spinel phase is more favored than other phases [54].

Since the discovery of the superconductivity in spinel $LiTi_2O_4$, much effort has been put into finding more spinel oxide superconductors. The studies of spinel oxide superconductors endeavored for the physics community for many years. The alternative view on the spinel superconductor, $LiTi_2O_4$, could be considered as the electron-doping in transition metal dichalcogenides, similar with Cu-doped $TiSe_2$. Li-doped anatase-$TiO_2$ crystallizes in tetragonal structure with the space group of $I4_1/amd$s. With doping more electrons into the system, the structural transitions happen from tetragonal to orthorhombic to cubic. The superconductivity was arisen when doping Li to ~1/2 per f.u. and the structure adopting to the cubic spinel. Similar structural transitions from tetragonal $I4_1/amd$ to F*d*-3*m* occur in another spinel superconductor, $CuIr_2S_4$ [55].

### 6.2. Superconductivity in non-oxide spinel $CuIr_2S_4$ and $CuV_2S_4$

$CuIr_2S_4$in the cubic structure with the space groupshows metallic properties at room temperature [56]. As the temperature decreases, $CuIr_2S_4$ undergoes a transition from a metal to an insulator around 230 K, which is also associated with a structural change from cubic to tetragonal [57]. Interestingly, a pseudogap is situated just above in the calculated density of states (DOS). In **Figure 5** (left), the DOS shows that ~6 eV range below the Fermi level ($E_F$) arises from all of the valence Cu, Ir and S orbitals. The contribution of Cu 4*s* and 3*d* electrons to the DOS curve, as shaded in **Figure 5** in black, states the filled-up *d* electrons are delocalized and hybridized with 5*d* electrons from Ir as well as 3*p* electrons from S, which is quite different from $LiTi_2O_4$. To further confirm our assumptions, the bonding/anti-bonding interactions (–COHP) in $CuIr_2S_4$ are calculated. Unlike the –COHP in $LiTi_2O_4$, which was dominated by Ti-O and Ti-Ti interactions, Ir-S and Cu-S interactions play the most important roles in the structural stabilization and superconducting properties in $CuIr_2S_4$. The band gap in $LiTi_2O_4$ corresponds to the non-bonding boundary in $LiTi_2O_4$; however, the 0–1 eV below the Fermi

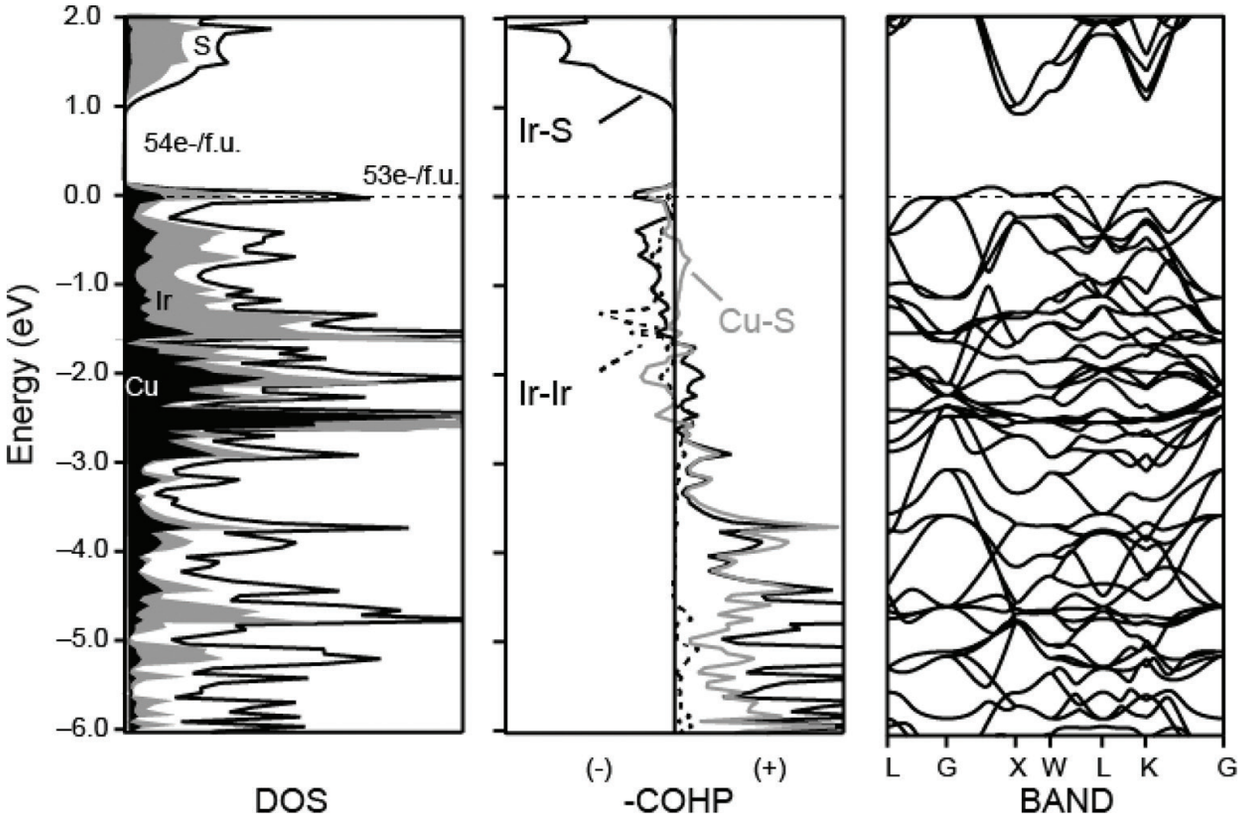


**Figure 5.** Electronic structure of spinel $CuIr_2S_4$. Partial DOS curves, –COHP curves and band structure of "$CuIr_2S_4$" obtained from non-spin-polarization (LDA). (+ is bonding/ – is anti-bonding, $E_F$ for $53e^-$ is set to zero).

level in $CuIr_2S_4$ is on the mixed status of Ir-S anti-bonding and Cu-S bonding interactions. The Fermi level at anti-bonding interactions indicates the instability of electronic structure of $CuIr_2S_4$ and the possible occurrence of superconductivity. The integrated DOS of $CuIr_2S_4$ gives 53e- per f.u., whereas the band gap just above Fermi level corresponds to 54e- per f.u., which can be expressed with the hypothetical compound "$CuIr_2S_4$(1e-)" according to the Zintl-Klemm concept. The ionic formula of $CuIr_2S_4$ can be interpreted as $Cu^{2+}(Ir^{3+})_2(S^{2-})_4$(1e-), the electron configuration of $Ir^{3+}$ becomes $5d^6$. Or $Cu^{+}(Ir^{4+})(Ir^{3+})(S^{2-})_4$(1e-) with two kinds of electron configurations of Ir, $5d^6$ and $5d^5$. The coordinated environment of $Ir^{3+}$ is octahedral ($O_h$), thus, the *d* orbital will split into $e_g$ and $t_{2g}$.

It has been well known even in textbooks that molecular transition metal complexes have a gap between the $e_g$ and $t_{2g}$ type in *d* orbitals, which is determined by the $\alpha$ and $\pi$ boning of the coordinated ligands. However, the band gap between the $e_g$ and $t_{2g}$ in *d* bands in certain solids is dependent on more complex orbital considerations. Take perovskite $LaCoO_3$ for example, the band gap is very small, close to 0 eV, but the iso-electronic $LaRhO_3$ has ~1.6 eV band gap. Similarly, in $CuIr_2S_4$, the band gap between $e_g$ and $t_{2g}$ is so small that the $5d^6$ and $5d^5$ configurations can coexist [58]. Moreover, at higher temperatures, a whole series of transformations take place triggered by thermal excitation of electrons from the valence to the conduction band. In $CuIr_2S_4$ compound, the two possible oxidation state fluctuations of $Cu^{+}/Cu^{2+}$ and $Ir^{3+}/Ir^{4+}$ could be related to superconductivity. The presence of a metal-insulator

(M-I) transition on cooling or under pressure has been of particular interest in the heavy metal chalcogenide spinel systems to make superconductors. Based on the decreased lattice parameters, $CuRh_2S_4$ and $CuRh_2Se_4$ can be treated as the compressed and expanded format of $CuIr_2S_4$ [59].

Another representative non-oxide spinel superconductor is $CuV_2S_4$ [60]. Unlike $CuIr_2S_4$, the superconductivity in $CuV_2S_4$ is induced by suppressing the CDWs rather than the metal-insulator transition in $CuIr_2S_4$ [61]. Also, according to the Zintl-Klemm concept, the ionic formula of $CuV_2S_4$ can be written as $Cu^{2+}(V^{3+})(V^{3+})(S^{2-})_4$. From the electronic structural calculations of $CuV_2S_4$ in **Figure 6**, a ~0.3 eV band gap is located at 0.6 eV below the Fermi level. The integrated DOS shows the gap responds to the 42e- (45e- for Fermi level). The band gap above Fermi level corresponds to 54e-, just as "$CuIr_2S_4$ (1e)." The band structure indicates the similarity between$CuV_2S_4$ (early transition metal, V) and $LiTi_2O_4$ (early transition metal, Ti) and the difference between $CuV_2S_4$ (early transition metal, V) and $CuIr_2S_4$ (late transition metal, Ir). By analogy with Jahn-Teller distortion ideas, the partially occupied bands are subject to the geometrical distortions related to a lowering of the total energy and usually termed as the instability of the Fermi surface (CDWs). A band gap may open at the Fermi level to create a semiconductor or insulator as the structure changes. From the chemistry viewpoint, the highest occupied conduction band is filled to make insulators. For example, in $MoS_2$, the charge density waves were observed in the localized unit of S-Mo-S rather than a localized

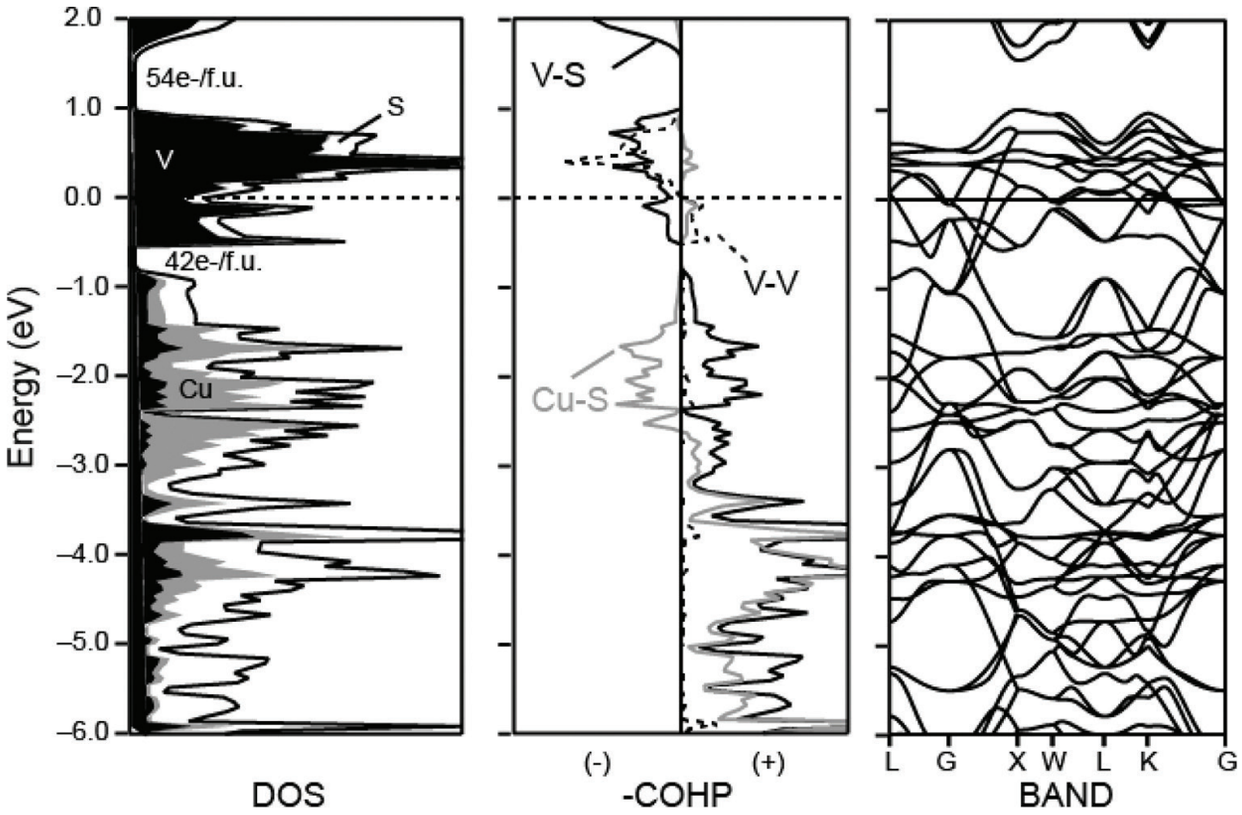


**Figure 6.** Electronic structure of spinel $CuV_2S_4$. Partial DOS curves,–COHP curves and band structure of "$CuV_2S_4$" obtained from non-spin-polarization (LDA). (+ is bonding/ – is anti-bonding, $E_F$ for $45e^-$ is set to zero).

atom. A series of superconductors were reported by suppression of the charge density waves in $MoS_2$, just like $CuV_2S_4$ [58].

Based on the above considerations, one of the most interesting areas from both chemical and physical points of view is identification of the factors that determines whether a particular solid is a conductor of electricity or a specific structure type is favored to hold the conducting properties and how well they do it. Furthermore, how external events such as pressure and temperature may affect a system to transit from one regime to the other. Are there any surprises associated with the transition between metal and insulator? Indeed, one of the consequences of the discovery of this series of superconducting copper and bismuth oxides has been unraveling of the possible connection with the metal-insulator transition. But what are the rules associated with the generation of this state of affairs, and what are the factors which compete with them and which lead to the superconductivity and how can we use this to make new superconductors? Recently, the superconductivity was observed in the non-superconducting $CuIr_2Se_4$ spinel by partial substitution of Pt for Ir [62].

## 7. Concluding remarks

The understanding of superconductivity from the viewpoint of chemistry offers a relatively straightforward approach to the real space rather than thinking in reciprocal space from a physical viewpoint. This chemical thinking is obviously basic, though not sufficiently comprehensive, as clearly shown by the competition between superconductivity and other structural phase transition (CDWs), oxidation fluctuation or magnetism. In this work, the introduced ideas are coming from the chemistry and carried some way into physics, alternatively, using chemical concepts to explain some physical phenomenon. A few questions arise about chemical trivial materials, such as how to make an indirect band gap a direct one. Several empirical rules can be used for chemists to design new superconductors.

1. Matthias' rule to make diamond-related $\alpha$-Mn type new superconductors: $\alpha$-Mn framework can be treated as defected 2 × 2 × 2 diamond structure shown in Xie's yet unpublished work. The space group of $\alpha$-Mn is I-43*m*, which is the direct subgroup of F*d*-3*m*. Re-rich binary compounds are favored by $\alpha$-Mn structure. By tuning the electron counts to 6.5e- per atom, $\alpha$-Mn type Re-rich compounds are highly likely to be superconductors.

2. Searching for the new pyrochlore-type superconductors: In a brief discussion of the structural chemistry of both cubic Laves phase and $Ni_2In$ structures, it is suggested that spinels and pyrochlores structures show the similarities just like cubic Laves phases and $Ni_2In$. Pyrochlores can be treated as the superlattice of spinels according to the connection in the lattice parameters. The superconductor, $Cd_2Re_2O_7$, in the pyrochlore-type structure can be conducted the similar research to $LiTi_2O_4$. Moreover, more non-oxide pyrochlore compounds can be synthesized to examine the superconducting properties.

3. It is not straightforward to predict the metallic or insulating properties, even harder to predict the M-I transition including the accompanying superconductivity sometimes.

But many CDW instabilities are triggered by lowering the temperature and occur in a range of systems, which cover a wide range of chemical types, including metal oxides and sulfides and molecular metals. The surprise of superconductivity may be observed by suppressing the CDWs.

## Acknowledgements

W. Xie thanks Louisiana State University for the start-up funding support and also acknowledges very helpful discussions with Professor Robert Cava (Princeton University) and Professor Gordon Miller (Iowa State University). W. Xie appreciates Yuze Gao for editing the references.

## Author details

Weiwei Xie[1]* and Huixia Luo[2]

*Address all correspondence to: weiweix@lsu.edu

1 Department of Chemistry, Louisiana State University, Baton Rouge, USA

2 Department of Chemistry, Princeton University, Princeton, USA

## References

[1] Meyers, H. P.; Myers, H. P. Introductory Solid State Physics, 2nd Edition; CRC Press, USA 1997.

[2] Larbalestier, D.; Gurevich, A.; Feldmann, D. M.; Polyanskii, A. Nature **2001**, 414 (6861), 368–377.

[3] Suhl, H.; Matthias, B. T.; Walker, L. R. Phys. Rev. Lett. **1959**, *3* (12), 552–554.

[4] Anderson, P. W. J.Phys.Chem.Solids **1959**, 11 (1), 26–30.

[5] Simon, A. Angew. Chem. Int. Ed. Engl. **1997**, 36 (17), 1788–1806.

[6] McMillan, W. L. Phys. Rev. **1968**, 167 (2), 331–344.

[7] Fässler, T. F.; Hoffmann, S. D. Angew. Chem. Int. Ed. Engl. **2004**, 43 (46), 6242–6247.

[8] Fredrickson, D. C.; Lee, S.; Hoffmann, R. Inorg. Chem. **2004**, 43 (20), 6159–6167.

[9] Xie, W.; Miller, G. J. Chem. Mater. **2014**, 26 (8), 2624–2634.

[10] Mizutani, U. Hume-Rothery Rules for Structurally Complex Alloy Phases; CRC Press, USA 2016.

[11] Xie, W.; Luo, H.; Phelan, B. F.; Klimczuk, T.; Cevallos, F. A.; Cava, R. J. PNAS **2015**, 112 (51), E7048–E7054.

[12] Miller, G. J. Eur. J. Inorg. Chem. **1998**, 1998 (5), 523–536.

[13] Matthias, B. T.; Geballe, T. H.; Compton, V. B. Rev. Mod. Phys. **1963**, 35 (1), 1–22.

[14] Matthias, B. T. Phys. Rev. **1955**, 97 (1), 74–76.

[15] Matthias, B. T.; Geballe, T. H.; Geller, S.; Corenzwit, E. Phys. Rev. **1954**, 95 (6), 1435–1435.

[16] Xie, W.; Luo, H.; Phelan, B. F.; Cava, R. J. J. Mater. Chem. C **2015**, 3 (31), 8235–8240.

[17] Xie, W.; Luo, H.; Seibel, E. M.; Nielsen, M. B.; Cava, R. J. Chem. Mater. **2015**, 27 (13), 4511–4514.

[18] Xie, W.; Fuccillo, M. K.; Phelan, B. F.; Luo, H.; Cava, R. J. J. Solid State Chem. **2015**, 227, 92–97.

[19] Snyder, G. J.; Toberer, E. S. Nat. Mater. **2008**, 7 (2), 105–114.

[20] Cava, R. J. Phys. C Superconductivity **1997**, 282, 27–33.

[21] Cava, R. J.; Batlogg, B.; van Dover, R. B.; Krajewski, J. J.; Waszczak, J. V. Nature **1990**, 345, 602–604.

[22] Takagi, H.; Cava, R. J.; Marezio, M.; Batlogg, B.; Krajewski, J. J.; Peck, W. F.; Bordet, P.; Cox, D. E. Phys. Rev. Lett. **1992**, 68 (25), 3777–3780.

[23] Cava, R. J. Chemistry of Bismuth and Lead based Superconducting Perovskites. United States: American Ceramic Society Inc.,1990.

[24] Kauzlarich, S. M.; Brown, S. R.; Snyder, G. J. Dalton Trans. **2007**, 21, 2099–2107.

[25] Schäfer, H.; Eisenmann, B.; Müller, W. Angew. Chem. Int. Ed. Engl. **1973**, 12 (9), 694–712.

[26] Cava, R. J.; Batlogg, B.; Krajewski, J. J.; Farrow, R.; Rupp, L. W.; White, A. E.; Short, K.; Peck, W. F.; Kometani, T. Nature **1988**, 332 (6167), 814–816.

[27] Cava, R. J.; Siegrist, T.; Peck, W. F.; Krajewski, J. J.; Batlogg, B.; Rosamilia, J. Phys. Rev. B **1991**, 44 (17), 9746–9748.

[28] Retoux, R.; Studer, F.; Michel, C.; Raveau, B.; Fontaine, A.; Dartyge, E. Phys. Rev. B **1990**, 41 (1), 193–199.

[29] Goodenough, J. B. Rep. Prog. Phys. **2004**, 67 (11), 1915.

[30] Timusk, T.; Statt, B. Rep. Prog. Phys. **1999**, 62 (1), 61.

[31] Mattheiss, L. F.; Hamann, D. R. Phys. Rev. B **1983**, 28 (8), 4227–4241.

[32] Hosono, H.; Tanabe, K.; Takayama-Muromachi, E.; Kageyama, H.; Yamanaka, S.; Kumakura, H.; Nohara, M.; Hiramatsu, H.; Fujitsu, S. Sci. Technol. Adv. Mater. **2015**, 16 (3), 33503.

[33] Cava, R. J.; Takagi, H.; Zandbergen, H. W.; Krajewski, J. J.; Peck, W. F.; Siegrist, T.; Batlogg, B.; van Dover, R. B.; Felder, R. J.; Mizuhashi, K.; Lee, J. O.; Eisaki, H.; Uchida, S. Nature **1994**, 367 (6460), 252–253.

[34] Miller, G. J. Am. Chem. Soc. 1994, **116**, 63324336.

[35] Montorsi, A. The Hubbard Model: A Reprint Volume; World Scientific, Singapore 1992.

[36] Compton, V. B.; Matthias, B. T. Acta Crystallogr. **1959**, 12 (9), 651–654.

[37] Blöchl, P. E.; Jepsen, O.; Andersen, O. K. Phys. Rev. B **1994**, 49 (23), 16223.

[38] Andersen, O. K.; Jepsen, O. Phys. Rev. Lett. **1984**, 53 (27), 2571–2574.

[39] Glötzel, D.; Segall, B.; Andersen, O. K. Solid State Commun. **1980**, 36 (5), 403–406.

[40] Becke, A. D. J.Chem. Phys. **1993**, 98 (2), 1372–1377.

[41] Methfessel, M.; Rodriguez, C. O.; Andersen, O. K. Phys. Rev. B **1989**, 40 (3), 2009–2012.

[42] Monkhorst, H. J.; Pack, J. D. Phys. Rev. B **1976**, 13 (12), 5188–5192.

[43] Dronskowski, R.; Bloechl, P. E. J. Phys. Chem. **1993**, 97 (33), 8617–8624.

[44] Schwarz, K.; Blaha, P. Comput. Mater. Sci. **2003**, 28 (2), 259–273.

[45] Schwarz, K. J. Solid State Chem. **2003**, 176 (2), 319–328.

[46] Perdew, J. P.; Burke, K.; Ernzerhof, M. Phys. Rev. Lett. **1996**, 77 (18), 3865–3868.

[47] Blaha, P.; Schwarz, K.; Sorantin, P.; Trickey, S. B. Comp. Phys. Commun. **1990**, 59 (2), 399–415.

[48] Jain, A.; Ong, S. P.; Hautier, G.; Chen, W.; Richards, W. D.; Dacek, S.; Cholia, S.; Gunter, D.; Skinner, D.; Ceder, G.; Persson, K. A. APL Mater. **2013**, 1 (1), 11002.

[49] Cava, R. J.; Murphy, D. W.; Zahurak, S.; Santoro, A.; Roth, R. S. J. Solid State Chem. **1984**, 53 (1), 64–75.

[50] Johnston, D. C.; Prakash, H.; Zachariasen, W. H.; Viswanathan, R. Mater. Res. Bull. **1973**, 8 (7), 777–784.

[51] Morosan, E.; Zandbergen, H. W.; Dennis, B. S.; Bos, J. W. G.; Onose, Y.; Klimczuk, T.; Ramirez, A. P.; Ong, N. P.; Cava, R. J. Nat. Phys. **2006**, 2 (8), 544–550.

[52] Burdett, J. K. Acta Cryst. Sect. B Struct. Sci. **1995**, 51 (4), 547–558.

[53] Hoffmann, R. Acc. Chem. Res. **1971**, 4 (1), 1–9.

[54] Murphy, D. W.; Sunshine, S.; van Dover, R. B.; Cava, R. J.; Batlogg, B.; Zahurak, S. M.; Schneemeyer, L. F. Phys. Rev. Lett. **1987**, 58 (18), 1888–1890.

[55] Nagata, S.; Hagino, T.; Seki, Y.; Bitoh, T. Phys. B Condens. Matter **1994**, 194, 1077–1078.

[56] Radaelli, P. G.; Horibe, Y.; Gutmann, M. J.; Ishibashi, H.; Chen, C. H.; Ibberson, R. M.; Koyama, Y.; Hor, Y.-S.; Kiryukhin, V.; Cheong, S.-W. Nature **2002**, 416 (6877), 155–158.

[57] Robbins, M.; Willens, R. H.; Miller, R. C. Solid State Commun. **1967**, 5 (12), 933–934.

[58] Burdett, J. K. Chem. Soc. Rev. **1994**, 23 (5), 299–308.

[59] Tachibana, M. Solid State Commun. **2012**, 152 (10), 849–851.

[60] Okada, H.; Koyama, K.; Watanabe, K. the AIP Conference Proceedings **2006**, 850, 1317–1318.

[61] Fleming, R. M.; DiSalvo, F. J.; Cava, R. J.; Waszczak, J. V. Phys. Rev. B **1981**, 24 (5), 2850–2853.

[62] Luo, H.; Klimczuk, T.; Müchler, L.; Schoop, L.; Hirai, D.; Fuccillo, M. K.; Felser, C.; Cava, R. J. Phys. Rev. B **2013**, 87 (21), 214510.